

# Large quasiparticle thermal Hall conductivity in the superconductor $\text{Ba}_{1-x}\text{K}_x\text{Fe}_2\text{As}_2$ .

J. G. Checkelsky<sup>1</sup>, Lu Li<sup>1,†</sup>, G. F. Chen<sup>2</sup>, J. L. Luo<sup>2</sup>, N. L. Wang<sup>2</sup> and N. P. Ong<sup>1</sup>

<sup>1</sup>*Department of Physics<sup>1</sup>, Princeton University, New Jersey 08544, U.S.A.*

<sup>2</sup>*Inst. of Physics, Beijing, China*

(Dated: November 30, 2008)

Both the thermal conductivity  $\kappa_{xx}$  and thermal Hall conductivity  $\kappa_{xy}$  in  $\text{Ba}_{1-x}\text{K}_x\text{Fe}_2\text{As}_2$  display large peak anomalies in the superconducting state. The anomalies imply that a large hole-like quasiparticle (qp) population exists below the critical temperature  $T_c$ , consistent with either a highly anisotropic gap or a gap with nodes. The curves of  $\kappa_{xx}$  measured to 35 T fit well to a vortex-scattering expression. The qp mean-free-path inferred reproduces the observed anomaly in  $\kappa_{xy}$ . Both channels provide a consistent estimate of a large qp population below  $T_c$ .

The discovery [1, 2, 3, 4, 5] of superconductivity in the iron pnictides has galvanized intense interest in this new class of superconductors. The highest critical temperature  $T_c$  achieved to date is  $\sim 55$  K in the (1111) family. Superconductivity has also been found in the 122 iron pnictides based on FeAs and FeSe [6]. As in the cuprates, one of the key issues is the gap symmetry. Nuclear magnetic resonance (NMR) relaxation experiments [7] are nominally consistent with nodes in the gap. However, angle-resolved photoemission spectroscopy (ARPES) experiments on  $\text{Ba}_{1-x}\text{K}_x\text{Fe}_2\text{As}_2$  [8, 9] favor isotropic gaps on the hole  $\Gamma$  Fermi Surface (FS), but the question of gap anisotropy is far from decided, especially on the sheets surrounding  $M$ .

If the gap parameter  $\Delta(\mathbf{k})$  is isotropic on each FS sheet, the population of Bogoliubov quasiparticles decreases sharply below  $T_c$  ( $\mathbf{k}$  is a wavevector on the FS). By contrast, if the nodes exist in  $\Delta(\mathbf{k})$  (or if  $|\Delta(\mathbf{k})|$  is strongly anisotropic), the quasiparticle (qp) population decreases quite gradually. In superconductors with unconventional gap symmetry, the thermal Hall conductivity  $\kappa_{xy}$  has proved to be a powerful probe for quasiparticles (qps). Unlike the diagonal thermal conductivity  $\kappa_{xx}$  which is the sum of the electronic term  $\kappa_e$  and the phonon term  $\kappa_{ph}$ , the off-diagonal term  $\kappa_{xy}$  is purely electronic. Together,  $\kappa_{xx}$  and  $\kappa_{xy}$  have been used to probe extensively the qp density and their lifetime in the cuprate  $\text{YBa}_2\text{Cu}_3\text{O}_y$  (YBCO) [10, 11, 12] and the heavy fermion superconductor  $\text{CeCoIn}_5$  [13, 14]. By contrast,  $\kappa_{xx}$  decreases roughly linearly with  $(T_c - T)$  below  $T_c$  in the clean  $s$ -wave superconductors Pb, Hg and Sn [15, 16] (data on  $\kappa_{xy}$  are unavailable).

We report detailed measurements of  $\kappa_{xx}(T, H)$  and  $\kappa_{xy}(T, H)$  on single crystals of  $\text{Ba}_{1-x}\text{K}_x\text{Fe}_2\text{As}_2$  in the geometry with the field  $\mathbf{H} \parallel \hat{\mathbf{z}} \parallel \hat{\mathbf{c}}$  and  $-\nabla T \parallel \hat{\mathbf{x}}$ . The longitudinal and transverse temperature gradients  $\delta T_x$  and  $\delta T_y$ , respectively, were measured using chromel-alumel thermocouples. The 2 crystals studied have dimensions  $2 \times 1 \times 0.1 \text{ mm}^3$ . At 10 K, the resolution achieved is  $\delta T_y \sim 10 \text{ mK}$ . Measurements of  $\kappa_{xy}$  were made to a maximum field of 14 Tesla using thermocouples. To extend measurements of  $\kappa_{xx}$  below 6 K where the thermocouple sensitivity falls steeply, we used matched  $\text{RuO}_x$  micro-sensors which are especially sensitive below 4 K (these measurements were performed to  $H = 35 \text{ T}$ ).

In the Boltzmann theory approach,  $\kappa_e$  from qp excitations is given by [15, 16]

$$\kappa_e = \frac{4}{T} \sum_{\mathbf{k}} \left( -\frac{\partial f_0}{\partial E_{\mathbf{k}}} \right) E_{\mathbf{k}}^2 v_x(\mathbf{k})^2 \tau(\mathbf{k}), \quad (1)$$

where  $E_{\mathbf{k}} = \sqrt{\Delta(\mathbf{k})^2 + \epsilon_{\mathbf{k}}^2}$  is the qp energy with  $\epsilon_{\mathbf{k}}$  the normal-state energy. Here,  $\mathbf{v}(\mathbf{k})$  is the qp group velocity,  $f_0$  the Fermi-Dirac distribution and  $\tau(\mathbf{k})$  the transport relaxation time. A recent treatment of  $\kappa_{xy}$  applied to YBCO is given by Durst *et al.* [17].

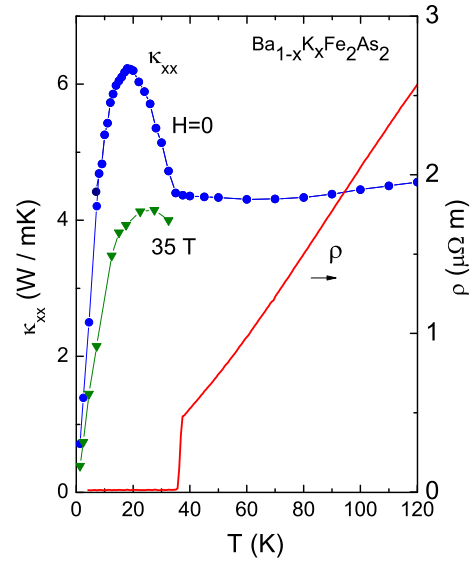


FIG. 1: The thermal conductivity  $\kappa_{xx}$  of single-crystal  $\text{Ba}_{1-x}\text{K}_x\text{Fe}_2\text{As}_2$  at  $H = 0$  (circles) and at 35 T (triangles). The solid curve is the in-plane resistivity  $\rho$  in zero  $H$  ( $T_c = 37 \text{ K}$ ).

Figure 1 plots the  $T$  dependence of  $\kappa_{xx}(T, H)$  in Sample 1 with  $H = 0$  (circles) and with  $H = 35 \text{ T}$  (triangles), together with the in-plane resistivity  $\rho$  (solid curve). The curve for  $\kappa_{xx}(T, 0)$  is closely similar in Sample 2. As shown,  $\kappa_{xx}(T, 0)$  is nearly  $T$  independent between  $T_c (= 37 \text{ K})$  and 100 K. Below  $T_c$ , it rises to a broad maximum that peaks near  $\frac{1}{2}T_c$ . In a 35-Tesla field, the anomaly is almost completely suppressed. Both the anomaly profile and its field suppression are similar to features seen in

YBCO and CeCoIn<sub>5</sub>. In these unconventional superconductors,  $\kappa_{xx}$  also rises to a large peak near  $\frac{1}{2}T_c$ , reflecting a large qp population and a greatly enhanced (zero-field) qp mean-free-path  $\ell_0$ .

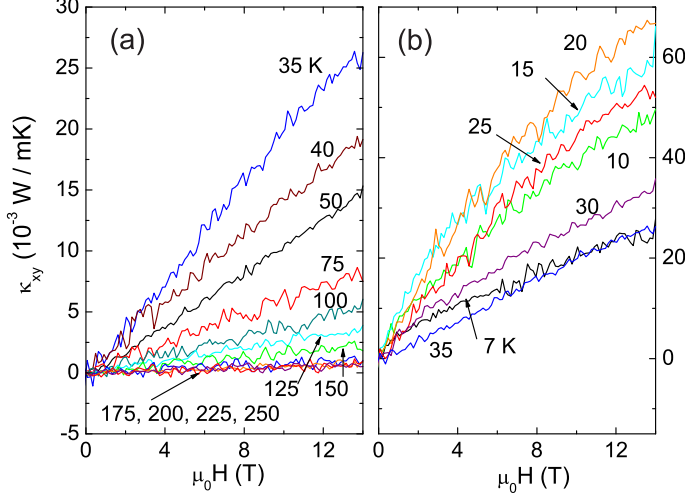


FIG. 2: Curves of the thermal Hall conductivity  $\kappa_{xy}$  vs.  $H$  in Ba<sub>1-x</sub>K<sub>x</sub>Fe<sub>2</sub>As<sub>2</sub> at  $T = 250 \rightarrow 35$  K (Panel a) and from  $35 \rightarrow 7$  K (b). Above  $T_c$  (37 K),  $\kappa_{xy}$  is  $H$  linear up to 14 T, but as  $T$  decreases below  $T_c$ , curvature becomes increasingly apparent (Panel b). At all  $T$ , the Hall signal is hole-like.

The curves of  $\kappa_{xy}$  vs.  $H$  at fixed  $T$  are displayed in Fig. 2. Both above and below  $T_c$ , the sign of  $\kappa_{xy}$  is positive (hole-like). Above  $T_c$ ,  $\kappa_{xy}$  is strictly linear in  $H$  (up to 14 T). As  $T$  decreases from 100 K to  $T_c$ , the slope of  $\kappa_{xy}$  vs.  $H$  increases gradually until  $T_c$ , where it undergoes a sharp increase.

In the normal state,  $\kappa_{xy}$  originates from the Lorentz force acting on the charge carriers (the Hall effect is also hole-like). Below  $T_c$ , the scattering of qps from pinned vortex lines possesses a right-left asymmetry which leads to a large  $\kappa_{xy}$  [10, 17, 18]. The asymmetry originates from the circulation of the supercurrent around the vortex core and the Volovik effect. The qp Hall current initially scales linearly with the vortex line density  $n_V = |B|/\phi_0$ , where  $B$  is the flux density and  $\phi_0$  the superconducting flux quantum. At large  $B$ , however, vortex scattering also severely reduces the mean-free-path of the qps (see below), resulting in a negative curvature in  $\kappa_{xy}(H)$ . In Fig. 2b, the steady increase in curvature is clearly seen as  $T$  decreases from 20 to 7 K.

Focussing on the weak- $H$  regime, we see that the sharp change at  $T_c$  in the qp Hall conductivity  $\kappa_{xy}$  becomes apparent when we plot the weak-field slope  $\kappa'_{xy0} \equiv \lim_{H \rightarrow 0} \kappa_{xy}/H$  (solid circles in Fig. 3). As  $T$  decreases from 200 K to  $T_c$ ,  $\kappa'_{xy}$  increases slowly by a factor of  $\sim 3$ . At  $T_c$ ,  $\kappa'_{xy0}$  exhibits a sharp break in slope followed by a much steeper rise to a peak that is  $\sim 5$  times larger than its value at  $T_c$  (we discuss the curves of  $A\kappa_e\alpha$  and  $\kappa_e$  below).

We next turn to the diagonal term  $\kappa_{xx}(T, H)$ , which

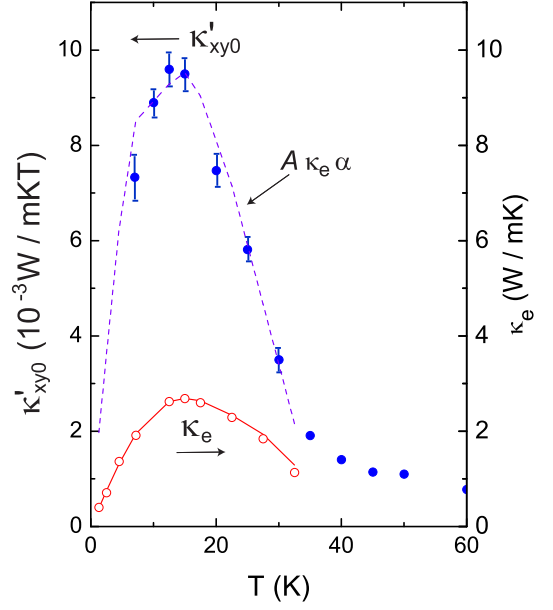


FIG. 3: The  $T$  dependence of the weak-field slope  $\kappa'_{xy0} \equiv \lim_{H \rightarrow 0} \kappa_{xy}/H$  (solid circles with error bars). As  $T$  falls below  $T_c$ ,  $\kappa'_{xy0}$  displays a steep increase to reach a peak at 18 K, reminiscent of the behavior in YBa<sub>2</sub>Cu<sub>3</sub>O<sub>7</sub>. For comparison, the quantity  $A\alpha\kappa_e$  (with  $A = 0.033$ , see below) is plotted as the dashed curve, and the electronic term  $\kappa_e$ , inferred from Eq. 2, is displayed as open circles.

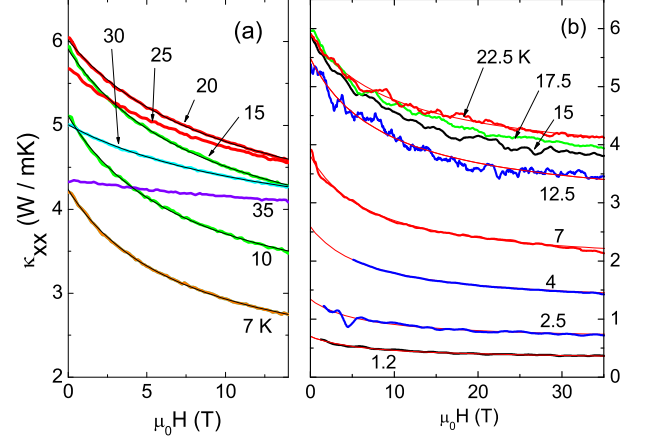


FIG. 4: Curves of  $\kappa_{xx}$  vs.  $H$  at fixed  $T$  measured with thermocouples to 14 T (Panel a) and with RuO<sub>x</sub> sensors to 35 T (b). Panel (a) shows in expanded scale the singular  $H$  dependence at  $T$  below  $T_c$  (37 K). Panel (b) displays measurements extended to  $H = 35$  T and to  $T = 1.2$  K. In both panels, fits to Eq. 2 are shown as thin curves.

provides quantitative estimates of the electronic term  $\kappa_e$  and  $\ell_0$  independent of  $\kappa_{xy}$  (Fig. 4). In the normal state, over the interval 250 to 40 K, the field dependence of  $\kappa_{xx}$  is undetectable with our sensitivity. Just below  $T_c$ , a weak  $H$  dependence becomes apparent (curve at 35 K Panel (a)). As  $T$  decreases, this rapidly evolves to a singular  $|B|$  dependence that characterizes the scattering

of qps from pinned vortices in type-II superconductors in the clean limit ( $\ell_0 \gg \xi$ , where  $\xi$  is the coherence length). In Panel (a), the measurements of  $\kappa_{xx}$  were made with thermocouples to  $H = 14$  T. The measurements were extended to lower  $T$  (1.2 K) and higher  $H$  (35 T) by the use of matched  $\text{RuO}_x$  micro-sensors (Fig. 4b).

The data in both panels of Fig 4 fit very well to the vortex-scattering expression (shown as thin curves) [10, 17, 18]

$$\kappa_{xx}(T, B) = \frac{\kappa_e(T)}{1 + \alpha(T)|B|} + \kappa_{ph}(T), \quad (2)$$

where  $\alpha(T) = \ell_0 \sigma_{tr} / \phi_0$  with  $\sigma_{tr}$  the vortex cross-section presented to an incident qp. Equation 2 expresses the additivity of the zero- $H$  scattering rate ( $\sim \ell_0^{-1}$ ) and the scattering rate introduced by vortices  $\ell_v^{-1} = \sigma_{tr} n_V$ . Because  $H_{c2} > 80$  T, the condensate amplitude is nearly unaffected by the applied  $H$ . Hence it is safe to assume that  $\kappa_e(T)$  is nearly independent of  $H$ , and the dominant contribution to the observed  $H$  dependence arises from vortex scattering. We have assumed that the phonon term  $\kappa_{ph}$  has negligible  $H$  dependence, consistent with  $q\xi \ll 1$ , where  $q$  is the average phonon wavevector for  $T < T_c$ .

From the fits to the curves in Fig. 4, we have determined  $\kappa_e(T)$ ,  $\kappa_{ph}(T)$  and  $\alpha(T)$ . These values are plotted in Figs. 5a and 5b, respectively. As shown in Panel (a), the phonon term  $\kappa_{ph}$  (open triangles) decreases monotonically as  $T$  decreases below  $T_c$ . By contrast, the zero- $H$  electronic term  $\kappa_e$  rises to a broad maximum at 15 K and then falls. As evident, the monotonic profile of  $\kappa_{ph}$  implies that the peak in  $\kappa_{xx}$  (in zero  $H$ ) is entirely associated with  $\kappa_e$ . In turn, the large peak in  $\kappa_e$  demands a large qp population that survives to  $\sim \frac{1}{2}T_c$ . We note that, above  $T_c$ ,  $\kappa_e$  accounts for less than  $\frac{1}{5}\kappa_{xx}$ , a fraction similar to that in YBCO [19].

The fits also yield estimates of  $\alpha = \ell_0 \sigma_{tr} / \phi_0$  which we display in Fig. 5b. As  $T$  decreases from 35 to 1.2 K,  $\alpha$  rises to  $3\times$  the value it had at  $T_c$ . This reflects primarily the increase in  $\ell_0$ . According to Cleary [18], the cross-section  $\sigma_{tr} \simeq \xi$ . With the estimate  $\xi \simeq 20$  Å (from  $H_{c2} \sim 85$  T), we find that  $\alpha$  at 1.2 K corresponds to  $\ell_0 \simeq 1,200$  Å. This supports our assumption that  $\text{Ba}_{1-x}\text{K}_x\text{Fe}_2\text{As}_2$  is in the clean limit  $\ell_0 \gg \xi$ .

Since  $\kappa_e$  is proportional to  $\ell_0$ , a nominal picture of the  $T$  dependence of the qp population may be obtained from the ratio  $\kappa_e/\ell_0$ . This quantity is plotted as open triangles in Fig. 5b. Initially,  $\kappa_e/\ell_0$  is nominally  $T$ -independent, but decreases linearly with  $T$  below 13 K. The initial plateau is also seen in  $\kappa_e/\ell_0$  measured in 90-K YBCO [10].

The fits of  $\kappa_{xx}$  vs.  $H$  to Eq. 2 has allowed us to determine  $\kappa_e$ ,  $\kappa_{ph}$ , and  $\alpha$  independent of  $\kappa_{xy}$ . To show that these estimates are consistent with the thermal Hall conductivity, we note that  $\kappa'_{xy0} \sim \ell_0^2$  should share the same  $T$  dependence as  $\alpha\kappa_e \sim \ell_0^2$ , in the semi-classical approximation. In Fig. 3, we have plotted  $A\kappa_e\alpha$  with the scale-factor  $A = 0.033$  (dashed curve) to compare it

with the measured values of  $\kappa'_{xy0}$ . Within the uncertainty inherent in  $\kappa'_{xy0}$ , the  $T$  dependences may be seen to track each other quite well, especially between 12 and 35 K. Hence, both  $\kappa_{xx}$  and  $\kappa_{xy}$  provide evidence for a large hole-like qp population that persists down to  $T \sim \frac{1}{2}T_c$ . Moreover, the values of  $\alpha \sim \ell_0$  inferred from  $\kappa_{xx}$  give a consistent description of the  $T$  dependences of both  $\kappa_e$  and  $\kappa'_{xy0}$ .

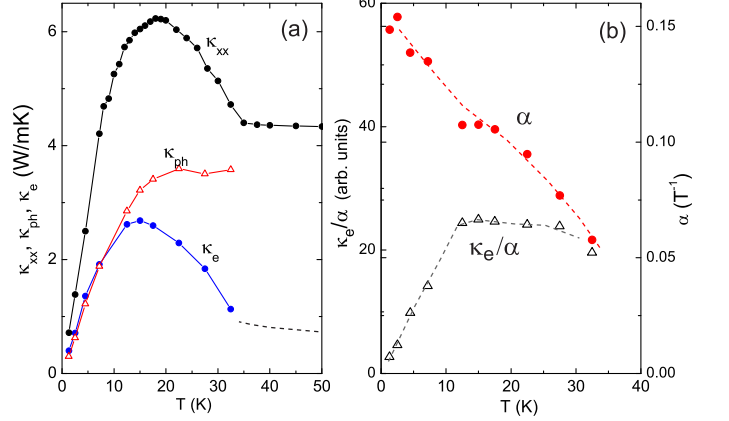


FIG. 5: (Panel a) Comparison of  $\kappa_{xx}$  with  $\kappa_e$  and  $\kappa_{ph}$  inferred from fits of curves in Fig. 4 to Eq. 2. Above  $T_c$ ,  $\kappa_e$  is less than  $\frac{1}{5}\kappa_{xx}$ . Below  $T_c$ , however,  $\kappa_e$  increases rapidly to account for the entire anomaly in the observed  $\kappa_{xx}$ . Panel (b) displays  $\alpha = \ell_0 \sigma_{tr} / \phi_0$  (solid circles) and  $\kappa_e/\alpha$  (open triangles) obtained from the fits. With  $\sigma_{tr} \sim 26$  Å, we estimate that  $\ell_0 \simeq 1,200$  Å at 2 K. The quantity  $\kappa_e/\alpha$  is a measure of the qp population below  $T_c$ .

We next discuss how disorder and inhomogeneities may affect these measurements. As these samples are first-generation crystals, disorder effects are a matter of experimental concern. Are the observed heat-transport anomalies an artifact of disorder? We argue that this possibility may be effectively excluded. As  $\kappa_{xy} \sim \ell_0^2$ , a decrease in  $\ell_0$  produced by additional scattering from impurities and lattice disorder strongly decreases  $\kappa_{xy}$  in the superconducting state. The trend has been confirmed repeatedly in earlier superconductors. In optimally-doped YBCO, the anomaly in  $\kappa_{xx}$  increases 3-fold in size when we compare the earliest twinned crystals with untwinned, high-purity crystals grown in BZO crucibles at Univ. British Columbia [12]. Values of  $\kappa_{xy}$  show an even larger increase. In  $\text{CeCoIn}_5$ , the  $\kappa_{xx}$  anomaly doubles in size between early crystals and later high-purity crystals [13, 14]. Instead of being the origin of these heat-transport anomalies, disorder actually suppresses them rapidly. We therefore conclude that they reflect the intrinsic qp properties of the pure system.

The value of  $\ell_0 \sim 1,200$  Å at 1.2 K – comparable with  $\ell_0$  observed in the earliest generations of YBCO crystals – is surprisingly long. It provides a measure of the length-scale of the electronic homogeneity in  $\text{Ba}_{1-x}\text{K}_x\text{Fe}_2\text{As}_2$ . The long  $\ell_0$  weakens significantly arguments advanced to explain, for e.g., the power-law decay of the NMR

relaxation by invoking strong disorder. This system lies in the opposite (clean) limit.

The abrupt increase in  $\ell_0(T)$  at  $T_c$  is similar to that observed in YBCO [10, 12]. In both systems, the increase seems too abrupt to be explained by the reduction in phase space for qp scattering caused by the opening of a strongly anisotropic gap. We raise the question whether this reflects the abrupt change of electron-electron interaction caused by the onset of long-range phase coherence at  $T_c$ . This issue, never resolved in cuprates, has again become important in the pnictides.

The symmetry of the gap in the iron pnictides has been the subject of considerable debate. The NMR relaxation rate  $1/(T_1T)$  in  $\text{LaFeAs}(\text{O}_{1-x}\text{F}_x)$  [7] follows a power-law relaxation rate extending over 3 decades in  $T$ . Because an isotropic  $\Delta$  would predict a Hebel-Slichter peak followed by exponential decay, the power-law relaxation rate is evidence for nodes. In models in which  $\Delta(\mathbf{k})$  is positive on the  $\Gamma$ -FS and negative on  $M$ -FS (but otherwise isotropic), absence of the Hebel-Slichter peak may be explained, but the power law is problematical [20].

ARPES measurements on  $\text{Ba}_{1-x}\text{K}_x\text{Fe}_2\text{As}_2$  reveal 2 hole-like FS sheets around the point  $\Gamma$  and 2 electron sheets around  $M$ , broadly consistent with LDA (local density approximation) band-structure calculations [21]. Measurements by ARPES of the superconducting  $\Delta(\mathbf{k})$  [8, 9] yield a nominally isotropic gap on the 2 hole FS sheets at  $\Gamma$ . If the gaps on the  $\Gamma$ -FS sheets are indeed isotropic, we are left with the possibility that the qps inferred from heat transport reside on the electron sheets (the ARPES resolution is insufficient to rule out gap variation on the electron FS). The possibility

of strong amplitude variation in  $\Delta(\mathbf{k})$  when the FS approaches the region in which  $\Delta(\mathbf{k})$  changes sign has been proposed [22].

However, a new ARPES experiment has shown that the FS in  $\text{Ba}_{1-x}\text{K}_x\text{Fe}_2\text{As}_2$  may be quite different from LDA predictions. Instead of the simple electron sheet at  $M$ , Zabolotnyy *et al.* [23] recently observed a “propeller” shaped complex comprised of 5 FS sheets arrayed around the point  $X/Y$ . The 4 blades of the propeller correspond to hole ellipses while the cone corresponds to a circular electron FS. We reason that the existence of strong gap anisotropy on the hole sheets at  $X/Y$  will accommodate the large qp population, as well as the positive sign of  $\kappa_{xy}$ .

As more experimental probes are brought to bear on the superconducting state in this interesting correlated multi-band system, we expect the picture to evolve. The properties of the quasiparticles extracted from heat transport will be valuable for understanding the pairing mechanism.

We thank P. A. Lee, D.-H. Lee, B. A. Bernevig and M. Z. Hasan for helpful discussions. The research at Princeton is supported by U.S. National Science Foundation (NSF) under Grant DMR-0819860. Research at IOP is supported by NSFC, 973 project of MOST and CAS of China. High-field experiments were performed at the National High Magnetic Field Laboratory, Tallahassee, a national facility supported by NSF, the Dept. of Energy and the State of Florida.

<sup>†</sup>*Present address of LL:* Dept. of Physics, MIT, Cambridge, MA.

- 
- [1] Y. Kamihara *et al.*, J. Am. Chem. Soc. **130**, 3296 (2008);
  - [2] Z. A. Ren *et al.*, Chin. Phys. Lett. **25**, 2215 (2008).
  - [3] G. F. Chen *et al.*, Phys. Rev. Lett. **100**, 247002 (2008);
  - [4] X. H. Chen *et al.*, Nature (London) **453**, 761 (2008).
  - [5] C. de la Cruz *et al.*, Nature (London) **453**, 899 (2008).
  - [6] F. C. Hsu *et al.*, Proc. National Acad. Sciences **105**, 14262 (2008).
  - [7] Y. Nakai, K. Ishida, Y. Kamihara, M. Hirano, and H. Hosono, J. Phys. Soc. Japan **77**, 073701 (2008).
  - [8] H. Ding *et al.*, Europhys. Lett. **83**, 4701 (2008).
  - [9] L. Wray *et al.*, Phys. Rev. B **78**, 184508 (2008).
  - [10] K. Krishana, J. M. Harris and N. P. Ong, Phys. Rev. Lett. **75**, 3529 (1995).
  - [11] B. Zeini *et al.*, Phys. Rev. Lett. **82**, 2175 (1999).
  - [12] Y. Zhang *et al.*, Phys. Rev. Lett. **86**, 890 (2001).
  - [13] K. Izawa *et al.*, Phys. Rev. Lett. **87**, 057002 (2001).
  - [14] Y. Onose, N. P. Ong and C. Petrovic, Europhys. Lett. **80**, 37005 (2007).
  - [15] J. Bardeen, G. Rickayzen and L. Tewordt, Phys. Rev. **113**, 982 (1959).
  - [16] Ludwig Tewordt, Phys. Rev. **129**, 657 (1963).
  - [17] A. C. Durst, A. Vishwanath and P. A. Lee, Phys. Rev. Lett. **90**, 187002 (2003).
  - [18] Robert M. Cleary, Phys. Rev. **175**, 587 (1968).
  - [19] Y. Zhang, N. P. Ong, Z. A. Xu, K. Krishana, R. Gagnon, and L. Taillefer, Phys. Rev. Lett. **84**, 2219 (2000).
  - [20] Meera M. Parish, Jiangping Hu, and B. Andrei Bernevig, Phys. Rev. B **78**, 144514 (2008).
  - [21] D. J. Singh and M. H. Du, Phys. Rev. Lett. **100**, 237003 (2008).
  - [22] Fa Wang, Hui Zhai, Ying Ran, Ashvin Vishwanath, and Dung-Hai Lee, cond-mat arXiv:0807.0498v4; K. Seo, B. A. Bernevig, and J. P. Hu, arXiv:0805.2958.
  - [23] V. B. Zabolotnyy *et al.*, cond-mat arXiv:0808.2454v2.